J Mater Sci (2006) 41:5263–5268
DOI 10.1007/s10853-006-0333-z

Low-cycle fatigue behavior of in situ TiB_2/Cu composite prepared by reactive hot pressing

S. C. Tjong · G. S. Wang

Received: 25 May 2004 / Accepted: 15 September 2005 / Published online: 27 May 2006

Abstract Copper-based composite reinforced with in situ TiB_2 particulates was prepared through reactive hot pressing of Ti, B and Cu powders. The formation of in situ TiB_2 particulates was verified by the X-ray diffraction technique. Tensile test showed that fine TiB_2 particulates were very effective to increase the tensile and yield strengths of copper at the expense of tensile ductility. Strain-controlled low-cycle fatigue measurements demonstrated that the in situ TiB_2/Cu composite exhibited essentially stable cyclic stress response behavior under small total strain amplitudes of 0.1–0.3%. However, this composite exhibited slight cyclic hardening under strain amplitude of 0.4%. Such cyclic hardening was more pronounced at a total strain amplitude to 0.6% due to the formation of dislocation cells and networks. Finally, the fatigue life data of the in situ TiB_2/Cu composite can be described by the Coffin–Manson equation.

Introduction

Metal matrix composites (MMCs) have emerged as an important class of structural materials because of their high strength and stiffness, good wear resistance and superior creep property. Continuous fiber reinforcement is known to provide the most effective strengthening, but particle reinforced composites are more attractive due to their cost-effectiveness and isotropic properties. Accordingly, MMCs find useful applications as light weight structural components in the automobile, aerospace and transport industries. Particulate-reinforced Al-based composites are regarded as good representatives of the MMCs, and their mechanical behavior has been extensively studied in the past decades.

In general, there are two processing routes to incorporate ceramic particulates into Al-based MMCs. The commonly used method involves the introduction of ceramic particulates into the matrices of MMCs via ingot casting or powder metallurgy (PM) process. The ceramic particulates are synthesized separately prior to composite fabrication. Such composites are termed as 'ex situ' MMCs in which agglomeration of fine ceramic particulates often occurs during processing. Another approach involves synthesizing the ceramic reinforcing phase directly within the matrix via reactive hot pressing (RHP) [1–4], and combustion synthesis techniques [4]. In the process, ultrafine ceramic particulates are formed in situ by the exothermic reaction between the element constituents of composites under hot pressing or combustion conditions. Such materials are termed as 'in situ' MMCs.

Because of excellent electric and thermal conductivities, copper has been widely used in industrial sectors. However, copper exhibits low mechanical strength that precludes it to be used as structural component materials. In order to improve mechanical strength, dispersion strengthened copper [5, 6] and ceramic particulate or whisker reinforced Cu matrix composites [7–12] were developed. Such ex situ copper-based composites exhibit an excellent combination of thermal and electrical conductivities, strength retention at elevated temperatures, and microstructural stability [5, 6, 12]. Among various ceramic reinforcements, titanium diboride (TiB_2) is particularly attractive because it exhibits high stiffness and hardness as

S. C. Tjong (✉) · G. S. Wang
Department of Physics and Materials Science, City University of Hong Kong, Tat Chee Avenue, Kowloon, Hong Kong
e-mail: aptjong@cityu.edu.hk

well as better electrical and thermal conductive in contrast to most ceramics. TiB_2 particulates can be formed in situ in the copper matrix via mechanical alloying (MA) [9] and RHP routes [13]. Biselli et al. have fabricated in situ TiB_2/Cu composite from Cu, Ti and B powder precursors using MA process followed by a suitable treatment. They reported that the in situ formed TiB_2 particulates are resistant to coarsening during annealing, thereby retaining the mechanical strength of the composite. Furthermore, the yield strength of in situ TiB_2/Cu composite is higher than that of the Al_2O_3/Cu dispersion alloy. The enhancement in yield strength results from good microstructural stability associated with chemical stability of the TiB_2 phase [9]. More recently, Ma and Tjong have prepared and investigated high temperature creep behavior of Cu-based MMC reinforced with in situ TiB_2 particulates via reactive hot pressing of Cu, Ti and B powders [13]. They reported that the creep resistance of in situ TiB_2/Cu composite is several orders of magnitude higher than that of pure copper.

As MMCs are potential structural materials for industrial applications, they are often subjected to cyclic deformation in addition to static mechanical stress. Thus the fatigue behavior of MMCs has attracted great interest of materials scientists. Ex situ SiC_p/Al composites are known to exhibit superior room-temperature fatigue endurance limit in high cycle fatigue (HCF) [14, 15], but not in low cycle fatigue (LCF) [16–22]. The improvement in the fatigue life of ex situ particulate reinforced Al-based MMCs under stress-controlled condition is attributed to an increase in fatigue strength. However, poor LCF life results from low ductility of the composites due to the incorporation of ceramic particulates. The strain-controlled LCF behavior of the copper-based MMCs reinforced either with ex situ or in situ ceramic particulates have received much less attention than that of the Al-based MMC counterparts. Gibeling and coworkers [23] have studied the LCF behavior of Al_2O_3 dispersion-strengthened copper alloy (GlidCop ZA-15). They reported that the dispersion-strengthened copper exhibits a relatively stable cyclic response at various plastic strain amplitudes. At low strain amplitudes, the fatigue lifetimes of the dispersion-strengthened copper and the base alloy are similar. However, the dispersion-strengthened copper is more susceptible to cracking at stress concentrations because of its substantially greater strength [23]. This paper aims to study the LCF behavior of in situ TiB_2/Cu composite prepared by RHP process.

Experimental procedure

Cu powder (99% purity, ≤74 μm), Ti powder (99% purity, 40 μm) and B powder (97% purity, ≤10 μm) were used as raw materials. The composition of these powders was adjusted so that 15 vol% TiB_2 were formed in situ, assuming that the reaction between Ti and B takes place completely. The fabrication process involved the initial ball milling of Cu, Ti and B powders, followed by cold compaction and reactive hot pressing of green billets at 1223 K in vacuum. The as-pressed billets were finally extruded into rods with an extrusion ratio of 20:1 at 1173 K. Pure Cu was also prepared under identical processing conditions. X-ray diffraction (XRD) and scanning electron microscopy (SEM) were employed to identify the structure and morphology of reinforcing phase developed in the composite.

Cylindrical specimens (4 mm diameter and 12.5 mm gauge length) for fatigue tests were machined from as-extruded bars with the loading axis parallel to the extrusion direction. The specimens were polished down to 1 μm diamond paste to remove the surface scratches. Fatigue tests were performed with a computer-controlled, closed-loop servohydraulic facility (Instron 8801) equipped with a 100 kN load cell under fully reversed axial tension–compression loading. The measurements were controlled under total strain amplitudes using a triangular push–pull wave shape and a constant nominal stain rate of 2×10^{-3} s^{-1}. The tests were continuously run to fracture of the specimens.

After fatigue test, thin slices were sectioned from the specimen gauge length. Disk specimens of 3 mm diameter were punched out and thinned by the ion beam until percolation occurred. The foils were examined in a Philips transmission electron microscope (CM20).

Results and discussion

Microstructure and tensile behavior

Figures 1 and 2 show the XRD pattern and SEM micrograph of in situ TiB_2/Cu composite formed by the RHP process. The in situ TiB_2 particulates exhibit irregular shape, and their sizes vary from 0. 167 to 4.24 μm. The size distribution of TiB_2 particulates determined from an image analyzer equipped with Leica QWin Plus software is shown in Fig. 3. Very few particles of 2–4 μm (less than 2%) are formed in situ during reactive hot pressing. The sizes of most TiB_2 particles are well below one micron as expected. The volume content of TiB_2 particles with sizes below 0.54 μm is 70.85 %. Such submicron particles can enhance the yield strength of the composite by means of the Orowan bowing mechanism. The tensile properties of the in situ TiB_2/Cu composite and unreinforced Cu at room temperature are listed in Table 1. It is apparent from this Table that the formation of fine TiB_2 particulates improves the yield and tensile strengths of Cu considerably at the expense of tensile ductility. This is the typical mechanical behavior of MMCs.

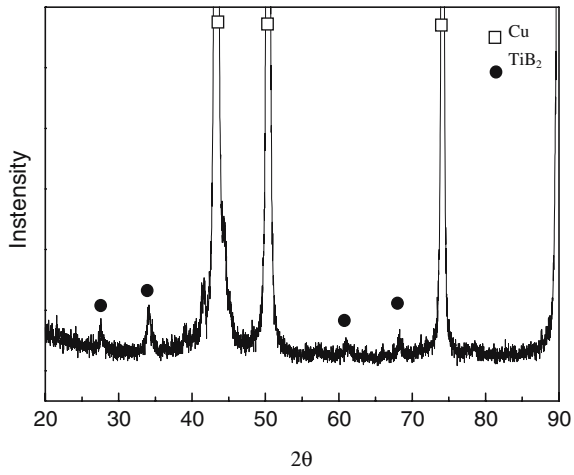

Fig. 1 XRD pattern of in situ TiB_2/Cu composite

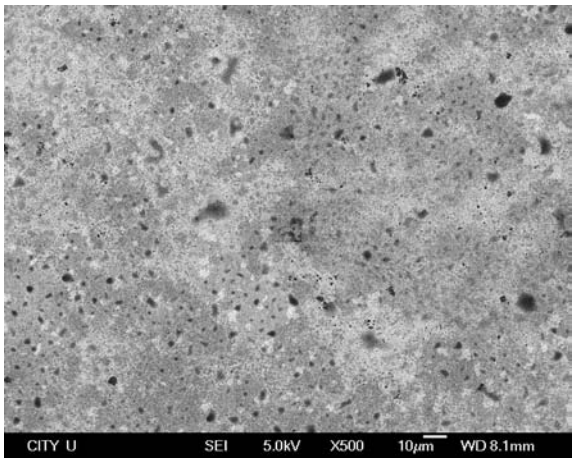

Fig. 2 SEM micrograph of in situ TiB_2/Cu composite

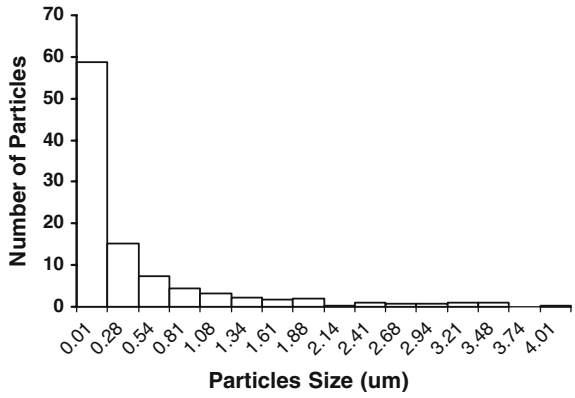

Fig. 3 Size distribution of in situ TiB_2 particles in Cu Matrix of in situ TiB_2/Cu composite determined from the image analysis

LCF cyclic stress response

Figure 4 shows the cyclic stress response curves of the in situ TiB_2/Cu composite under various total strain amplitudes. For the purpose of comparison, the cyclic stress response curves of pure Cu under fixed total strain amplitudes ($\Delta\varepsilon_t/2$) of 0.3% and 0.4% are shown in Fig. 5. The cyclic stress response was determined by monitoring the stress amplitude during strain-controlled fatigue measurements. The stress amplitude was taken as the average of the peak values of the stress in tension and in compression. In this regard, the cyclic stress response curves represent the variation of stress amplitude with number of cycles (N) at fixed total strain amplitudes. From Fig. 5, ductile and soft Cu exhibits cyclic hardening up to final fracture as

Table 1 Tensile properties of unreinforced Cu and TiB_2/Cu composite at room temperature

Materials	Elastic modulus (GPa)	UTS (MPa)	YS (MPa)	El. (%)
Cu	90	304.8	75.0	43.8
TiB_2/Cu	120	734.7	655.6	9.6

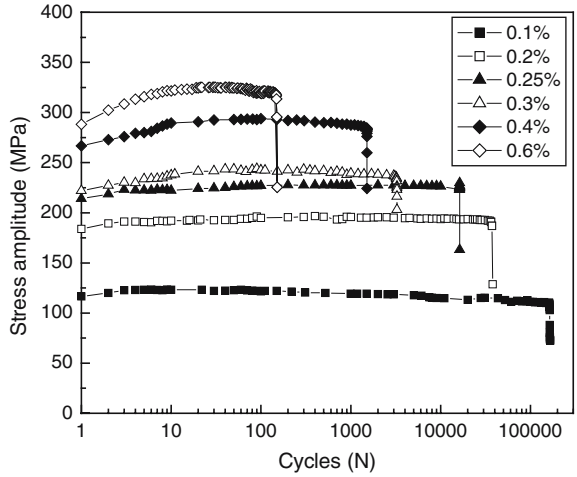

Fig. 4 Cyclic stress response of in situ TiB_2/Cu composite cycled at various total strain amplitudes

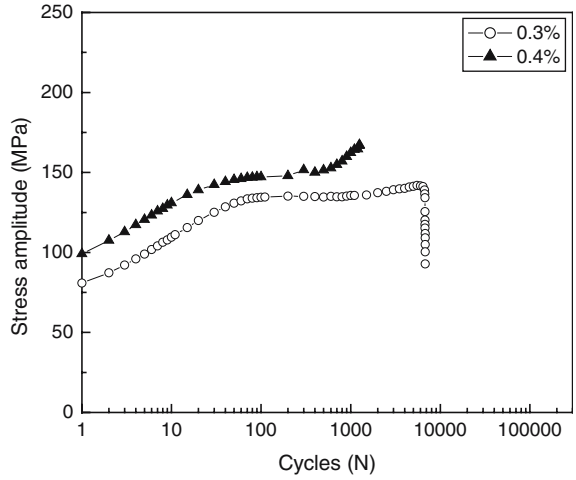

Fig. 5 Cyclic stress response of pure Cu composite cycled at total strain amplitudes of 0.3% and 0.4%

expected. In contrast, in situ TiB_2/Cu composite exhibits essentially stable cyclic behavior at low total strain amplitudes of 0.1–0.3%. This demonstrates that the composite exhibits no cyclic hardening or softening cycled at low strain amplitudes. However, the composite exhibits very slight hardening under a strain amplitude of 0.4%. Such cyclic hardening is more pronounced by increasing the strain amplitude to 0.6%. It is generally known that the cyclic strain hardening of pure Cu is derived from the generation, multiplication and interaction of dislocations during cyclic deformation. Such dislocations tend to arrange themselves into low energy dislocation structures such as loop patches and persistent slip bands [24–26]. Thus the dislocation structures generated during cycling can provide useful mechanistic information on the cyclic deformation of metals and composites. In this aspect, TEM is a powerful tool to observe the dislocation structures developed in metals during cycling.

Figure 6 shows a typical TEM micrograph of the in situ TiB_2/Cu composite prior to cycling. High density of dislocations is observed in the Cu matrix after extruding the TiB_2/Cu composite at 1173 K. The dislocations are generated upon cooling the in situ TiB_2/Cu composite from fabrication temperature due to a large difference in thermal expansion coefficients (CTE) between the TiB_2 ceramic reinforcement and copper matrix. The generation of dislocations in MMCs due to large CTE mismatch between the reinforcement and matrix is well documented in the literature [27]. On the other hand, new dislocations are developed in the TiB_2/Cu composite cycled at a strain amplitude of 0.4%. The dislocation motion is impeded by fine TiB_2 submicron particles. The dislocations appear as tangles and loop patches due to the interaction with fine TiB_2 particles (Fig. 7). At larger strain amplitude of 0.6%, bundles of loop patches link together to form the wall of dislocation cell (Fig. 8a) and dislocation networks (Fig. 8b, c). It is considered that cyclic hardening of the TiB_2/Cu composite deformed at strain amplitudes of 0.4% and 0.6% results from the dislocation multiplication and accumulation in the high stress regions near the particulates. As mentioned above, the size of in situ TiB_2 particulates varies from 0.167 to 4.25 μm. For the TiB_2 particulates with diameters smaller than 0.54 μm (70.85%) can act as obstacles for the dislocations during cycling. Such dislocation–ceramic particle interaction generally enhances the dislocation density. This leads to the cyclic hardening observed in the TiB_2/Cu composite cycled at strain amplitudes of 0.4% and 0.6%.

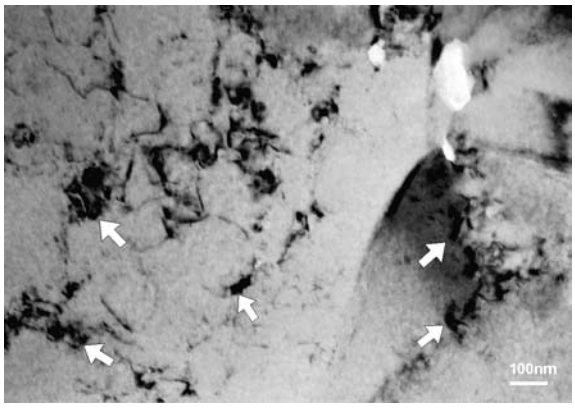

Fig. 6 TEM micrograph of undeformed TiB_2/Cu composite showing generation of dislocations due to large CTE mismatch between the reinforcement and the matrix. White arrows indicate in situ TiB_2 particles

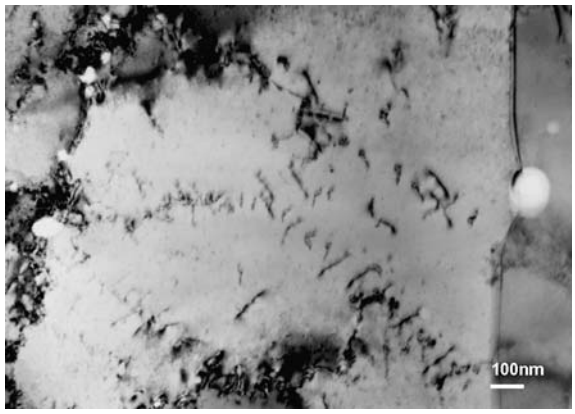

Fig. 7 TEM micrograph of in situ TiB_2/Cu composite deformed to failure at a strain amplitude of 0.4%

LCF life

The correlation between the cyclic plastic strain amplitude ($\Delta\varepsilon_p/2$), and the number of reversals to failure for the composites can be described by the Manson–Coffin relationship:

$$\frac{\Delta\varepsilon_p}{2} = \varepsilon_f'(2N_f)^C \quad (1)$$

where ε_f' is a fatigue ductility coefficient and c is a fatigue ductility exponent. The plastic strain range can be determined from the cyclic hysteresis loop according to the following relation:

$$\Delta\varepsilon_p = \Delta\varepsilon_t - \frac{\Delta\sigma}{E} \quad (2)$$

where E is Young's modulus, $\Delta\varepsilon_t$ the total strain range and $\Delta\sigma$ the applied stress range.

Figure 9 shows the plastic strain amplitude versus reversals to failure ($2N_f$) for in situ TiB_2/Cu composite investigated. Linear regression analysis was used to fit the experimental data for the Coffin–Manson plot. An extrapolation of the best fit is made to determine the value of cyclic

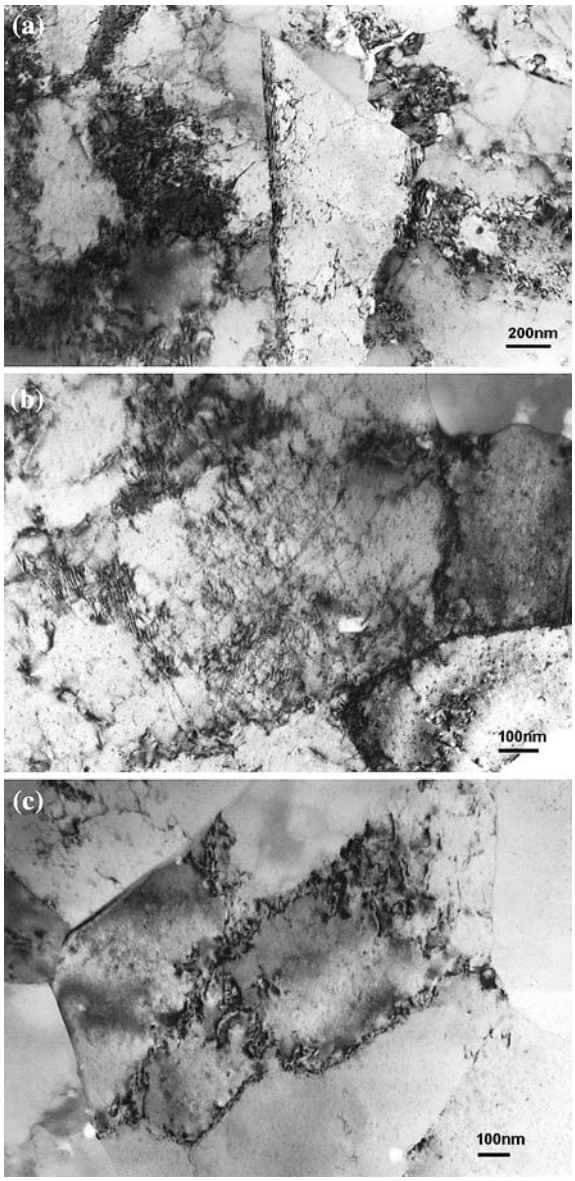

Fig. 8 (**a**) TEM micrograph of in situ TiB_2/Cu composite cycled to failure at a strain amplitude of 0.6% showing formation of dislocation cells. Dislocation tangles and loop patches near the grain-boundaries of a central grain can be readily seen; (**b**) and (**c**) other regions of the same specimen showing formation of the dislocation networks in Cu matrix

plastic strain at $2N_f = 1$. This corresponds to the fatigue ductility coefficient (ε_f') and is related to cyclic ductility of the material. The slope of the plot yields the fatigue ductility exponent (c). Figure 9 clearly indicates that the predicted fatigue lives coincide reasonably well with the experimental data over a wide range of plastic strain amplitudes. In the case of unreinforced copper, $\varepsilon_f'$is approximately equal to the true fracture strain (ε_f). The true fracture strain of metals can be related to engineering strain (ε_E) from

$$\varepsilon_f = \ln(1 + \varepsilon_E) \quad (3)$$

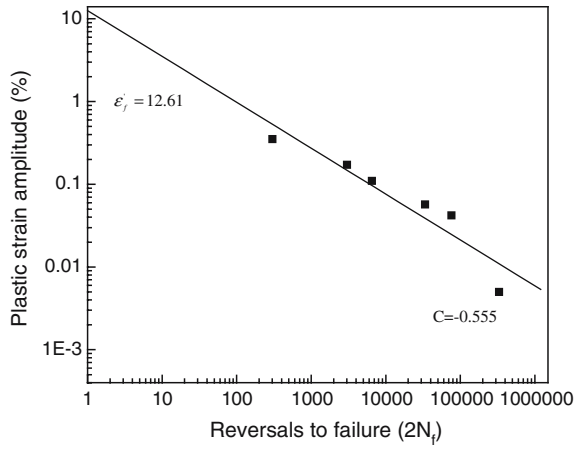

Fig. 9 Log–log plots of the plastic strain amplitude versus reversals to failure for in situ TiB_2/Cu composite

. Thus, the ε_f value of pure copper with ε_E of 43.8% (Table 1) is about 36.3%. From the Coffin–Manson plots, the TiB_2/Cu composite exhibits lower ε_f' value (12.61%) compared to pure Cu, implying this composite has lower LCF endurance than copper. This is as expected because the incorporation of ceramic particulates to metal matrices is known to reduce the tensile ductility or fracture strain of the metals. In other words, the formation of in situ TiB_2 particulates reduces the fatigue ductility of copper under strain-controlled LCF tests.

Conclusion

In situ TiB_2/Cu composite was successfully fabricated via reaction hot pressing of Ti, B and Cu powders. XRD and SEM were used to identify the formation of the in situ TiB_2 phase. Tensile test showed that the TiB_2 phase reinforced the copper matrix effectively at the expense of tensile ductility. Strain-controlled LCF measurements that the in situ TiB_2/Cu composite exhibited essentially stable cyclic stress response behavior under small total strain amplitudes of 0.1–0.3%. However, this composite exhibited very slight hardening under strain amplitude of 0.4%. Such cyclic hardening was more pronounced by increasing the strain amplitude to 0.6% and could be attributed to dislocation generation and multiplication during cyclic loading. This led to the formation of dislocation cells and networks. Finally, the fatigue life data of the in situ TiB_2/Cu composite can be described by the Coffin–Manson equation.

References

1. Ma ZY, Li JH, Li SX, Ning XG, Lu YX, Bi J (1996) J Mater Sci 31:741
2. Ma ZY, Tjong SC (1997) Metall Mater Trans 28A:1931

3. Tjong SC, Ma ZY (2000) Mater Sci Eng R 29:49
4. Kwon YJ, Kobashi M, Chon T, Kanetake N (2004) Scripta Mater 50:577
5. Nagorka MS, Levi CC, Lucas GE, Ridder SD (1991) Mater Sci Eng A 104:277
6. Groza JR, Gibeling JC (1993) Mater Sci Eng A 171:115
7. Joo LA, Tucker KW, Shaner JR (1986) US Pat 4617053
8. Perez JF, Morris DG (1994) Scripta Metall Mater 31:231
9. Biselli C, Morris DG, Randall N (1994) Scripta Metall Mater 30:1327
10. Chrysanthou A, Erbaccio G (1995) J Materr Sci 30:6339
11. Yih P, Chung DDL (1995) Int J Powder Metall 31:335
12. Yih P, Chung DDL (1997) J Mater Sci 32:1703
13. Ma ZY, Tjong SC (2000) Mater Sci Eng A 284:70
14. Srivatsan TS, Al-Hajri M, Petraoli M, Hotton B, Lam PC (2002) Mater Sci Eng A 325:202
15. Bonnen JJ, Allison JE, Jones JW (1991) Metall Mater Trans A 22:1007
16. Vyletel GM, van Aken DC, Allison JE (1991) Scripta Metall Mater 25:2405
17. LLorca J, Poza P (1995) Acta Metall Mater 43:3959
18. Han NL, Wang ZG, Sun LZ (1995) Scripta Metall Mater 32:1739
19. Han NL, Wang ZG, Sun LZ (1995) Scripta Metall Mater 33:781
20. Hadianfard MJ, Mai YW (2000) J Mater Sci 35:1715
21. Tjong SC, Wang GS, Mai YW (2003) Mater Sci Eng A 358:99
22. Tjong SC, Wang GS, Geng L, Mai YW (2004) Compos Sci Technol 64:1971
23. Robles J, Anderson KR, Groza JR, Gibeling JC (1994) Metall Mater Trans A 25:2235
24. Liu CD, Bassim MN, You DX (1994) Acta Metal Mater 42:3695
25. LLanes L, Rollett AD, Laird C, Bassani JL (1993) Acta Metal Mater 41:2667
26. Huang HL (2003) Mater Sci Eng A 342:38
27. Arsenault RJ, Shi N (1986) Mater Sci Eng A 81:175